Dear Editors and Referees:

Thank you very much for your careful review and helpful comments on our manuscript acp-2019-758. We have accordingly made the careful revisions. The revised portions are highlighted in the revised manuscript. In the following we quoted each review question in the square brackets and added our response after each paragraph.

Responses to Referee #1

[1. Lines 692-697: There are several typos here. "within," should be revised as period. Also, is "Thermo Fisher Scientifi" correct here? Please double check. Meanwhile, I suggest the authors add some references for using this instrument to measure PM over China.]

Response 1: We have revised the typos and removed the sentence with "Thermo Fisher Scientific", following the ACP requirements to cite the instrument (instruments maker) in the manuscript. Actually, the observation data of hourly $PM_{2.5}$ concentrations in this study were under quality control that is based on China's national standard of air quality observation operated by the Ministry of Ecology and Environment (http://www.mee.gov.cn/) .

[2. Lines 695-697: Should the "Ministry of ecology and environmental protection of China" be changed to "Ministry of Ecology and Environmental Protection of People's Republic of China"?]

Response 2: It has been changed.

[3. Line 916: change the "Meteorological" to "meteorological".]

Response 3: Thanks for the careful review. It has been changed.

[4. Phrases of "Central and Eastern China (CEC)" and "CEC" are used in the abstract. However, the authors use "Central-eastern China" in the main text. Please be consistent. I would suggest using "central-eastern China" across the entire manuscript, including the abstract.]

Response 4: Following the reviewer's suggestion, we have used "CEC" from the full Phrases of central-eastern China consistently in the abstract, the main text and the figure captions of the revised manuscript.

Responses to Referee #2

[1. Issue 1 related to manuscript-structure organization: P147-165, Section 2.2.2, the model simulation validation should be not presented here.]

Response 1: Many thanks for the referee's comment.

The FLEXPART model was coupled offline with the Weather Research and Forecasting (WRF) model to effectively devise the combined model FLEXPART-WRF (Fast and Easter, 2006; Brioude et al., 2013), which was used to characterize $PM_{2.5}$ sources and regional transport in this study. The the validation of Section 2.2.2 was only for the meteorology simulated by the WRF model, Because the WRF-simulated meteorology was used to drive the FLEXPART backward trajectory simulation, it could be better to present *Section 2.2.2,* the WRF modeling meteorological validation before Section 2.3, Estimating contribution of regional transport of $PM_{2.5}$ to air pollution based on the backward trajectory of FLEXPART-WRF modeling.

By the way, we have updated the subtitle of Section 2.2.2 with "WRF modeling configuration and meteorological validation" in the revised manuscript to avoid the misleading of readers.

[2. Issue 2 related to manuscript-structure organization: the three sections, i.e., Sections 3.2, 3.3, and 3.3 are presented in the current version to illustrate the impact of meteorological conditions such as winds and stabilities of the atmospheric boundary layer on surface PM2.5 concentrations and pollution events. I am not sure that the authors need three sub-sections to discuss them separately. To me, the observed evidence is pretty clear and straightforward that heavy PM2.5 pollution events (daily mean concentrations higher than 150.0 μg · *m!") were caused by strong northly winds and light pollution was associated with local sources. I would suggest combining them or re-organizing them further in a better way.]*

Response 2: Following the referee's suggestion, we have re-organized Section 3. Results and Discussion in the revised manuscript as follows:

1) Combining the old Section 3.1 and the first paragraph of old Section 3.2 into the new Section 3.1 with the updated subtitle of "**Variations in local $PM_{2.5}$ concentrations and meteorology in January 2016**".

2) Combining the the last paragraph of the old Section 3.2 and the old section 3.3 into the new Section 3.2 with the subtitle of "**A unique meteorological condition of "non-stagnation" for heavy $PM_{2.5}$ pollution"** and restructuring the new the new Section 3.2 into Section **3.2.1 Strong northerly winds and** Section **3.2.2 unstable structures in the atmospheric boundary layer.**

3) The subtitle of new Section 3.3 has been modified to "**Regional transport of $PM_{2.5}$ in northerly winds observed over CEC**".

4) The new Sections 3.4 was from the old Section 3.5.

[3. To better characterize the unique features of the ABL for the heavy pollution events in this region, the authors are suggested to shed more light on the characteristics of the ABL for different pollution events. Fig.6 is a good one but it isn't enough. For instance, which cases do the profiles presented in Fig.6 represent? What time and which day? If these profiles represented the conventional sounding data like twice a day (07am and 07 pm Beijing Time), that would be not sufficient. It will be very helpful if the authors can present any more observed profiles like LiDAR measurements, Wind Profilers data, etc. to compare the differences between the three heavy pollution events and a case with low PM2.5 as well as their evolution. Any effort like that will be a strong support to the conclusions that the authors want to draw through this study.]

Response 3: Many thanks for the referee's suggestions.

We understand that the unique features of the ABL could be better characterized for the heavy pollution events in this region with the fine data of vertical observations. However, there were no available LiDAR, Wind Profile and other observation data over the YRMB area in January 2016 for our study period, and we had to use the conventional sounding data of meteorology like twice a day (08am and 08 pm Beijing Time) to present the characteristics of the ABL structures for heavy pollution events and clean air period during January 2016. Because the heavy $PM_{2.5}$ pollution events were observed by short durations of less than 26 h from rapid accumulation to fast dissipation, we can not present the ABL vertical profiles for each heavy pollution event due to the no effective data of the conventional sounding observation, and Fig. 6 compared the vertical profiles of air temperature, wind velocity and potential temperature averaged in the heavy pollution periods P1, P2 and P3 and in the clean air period over Wuhan during January 2016 to exhibit the unique unstable ABL structures for heavy $PM_{2.5}$ pollution.

By the way, the caption of Fig. 6 has been clarified as "Fig. 6. Vertical profiles of (a) air temperature, (b) wind velocity and (c) potential temperature averaged in the heavy pollution periods P1, P2 and P3 and in the clean air period over Wuhan during January 2016." in the revised manuscript.

[4. English writing is another major concern that the authors really need more efforts. There are many writing issues related to grammar, typo, sentence structures, inappropriate words, etc. I am not going to list them here. My suggestion is to find a professional language edit service.]

Response 4: Following the referee's suggestion, the manuscript was edited by Elsevier Language Editing Services (please see the following Elsevier certificate)

.

Language Editing Services

Registered Office:
Elsevier Ltd
The Boulevard, Langford Lane,
Kidlington, OX5 1GB, UK.
Registration No. 331566771

To whom it may concern

The paper "Heavy air pollution with the unique “non-stagnant” atmospheric boundary layer in the Yangtze River Middle Basin aggravated by regional transport of PM2.5 over China" by Chao Yu was edited by Elsevier Language Editing Services.

Kind regards,

Elsevier Webshop Support

(This is a computer generated advice and does not require any signature)

Heavy air pollution with a unique "non-stagnant" atmospheric boundary layer in the Yangtze River Middle Basin aggravated by regional transport of $PM_{2.5}$ over China

Chao Yu[1,2], Tianliang Zhao[1, *], Yongqing Bai[3, *], Lei Zhang[1,4], Shaofei Kong[5], Xingna Yu[1], Jinhai He[1], Chunguang Cui[3], Jie Yang[1], Yinchang You[1], Guoxu Ma[1], Ming Wu[1], Jiacheng Chang[1]

1 Collaborative Innovation Center on Forecast and Evaluation of Meteorological Disasters, Key Laboratory for Aerosol-Cloud-Precipitation of China Meteorological Administration, PREMIC, Nanjing University of Information Science and Technology, Nanjing 210044, China

2 Southwest Electric Power Design Institute Co., Ltd of China Power Engineering Consulting Group, Chengdu, 610021, China

3 Institute of Heavy Rain, China Meteorological Administration, Wuhan, 430205, China

4 Chengdu Academy of Environmental Sciences, Chengdu, 610031, China

5 Department of Atmospheric Sciences, School of Environmental Studies, China University of Geosciences (Wuhan), 430074, Wuhan, China

* *Correspondence*: Tianliang Zhao (tlzhao@nuist.edu.cn); Yongqing Bai (2007byq@163.com)

Abstract: The regional transport of air pollutants, controlled by emission sources and meteorological factors, results in a complex source-receptor relationship of air pollution change. Wuhan, a metropolis in the Yangtze River Middle Basin (YRMB) of Central China, experienced heavy air pollution characterized by hourly $PM_{2.5}$ concentrations reaching 471.1 μg m^{-3} in January 2016. To investigate the regional transport of $PM_{2.5}$ over ~~C~~central~~ and ~~-~~E~~eastern China (CEC) and the meteorological impact on wintertime air pollution in the YRMB area, observational meteorological and other relevant environmental data from January 2016 were analyzed. Our analysis presented noteworthy cases of heavy $PM_{2.5}$ pollution in the YRMB area with unique "non-stagnant" meteorological conditions of strong northerly winds, no temperature inversion, and additional unstable structures in the atmospheric boundary layer. This unique set of conditions differed from the stagnant meteorological conditions characterized by near-surface weak winds, air temperature inversion, and stable structure in the boundary layer that are typically observed in heavy air pollution over most regions in China. The regional transport of $PM_{2.5}$ over CEC aggravated $PM_{2.5}$ levels, thus creating heavy air pollution in the YRMB area. This demonstrates a source-receptor relationship between the originating air pollution regions in CEC and the receiving YRMB region. Furthermore, a backward trajectory simulation using a FLEXPART-WRF model to integrate the air pollutant emission inventory over China was used to explore the patterns of regional transport of $PM_{2.5}$ governed by the strong northerly winds in the cold air activity of the East Asian winter monsoon season that contributes markedly to the heavy $PM_{2.5}$ pollution in the YRMB area. It was estimated that the regional transport of $PM_{2.5}$ from non-local air pollutant emissions contributes more than 65% of the $PM_{2.5}$ concentrations to the heavy air pollution in the YRMB region during the study period, revealing the importance of the regional transport of air pollutants over China as a causative factor of heavy air pollution over the YRMB area.

Key words: $PM_{2.5}$ pollution; Yangtze River Middle Basin; meteorological condition; regional transport; FLEXPART-WRF

1. Introduction

Haze pollution can result in serious environmental problems that adversely influence traffic, human health, climate change, and other significant aspects (An et al., 2019; Fuzzi et al., 2015; Nel, 2005). Based on observations in China, there is a well-established association between haze pollution and high concentrations of $PM_{2.5}$ (particulate matter with an aerodynamic diameter equal to or less than 2.5 μm). Air pollution levels are highly dependent on the emissions of air pollutants and changes in meteorology (An et al., 2019; Tie et al., 2017; Xu et al., 2016a; Xu et al., 2016b). The accumulation, maintenance, and dissipation of haze pollution events are generally determined by meteorological changes (Zhang et al., 2013; Zhang et al., 2015), among which boundary layer structures play the most important role (Zhao et al., 2013). Meteorological conditions of stagnation, characterized by near-surface low winds, high humidity, and stable boundary layers, could govern the periodic variations of haze pollution, which present as typical wintertime air pollution in China (Huang et al., 2018; Xu et al., 2016b; Zhang et al., 2013). Major anthropogenic pollutant sources exist over the vast flatland in ~~C~~central~~ and ~~-~~E~~eastern China (CEC), from the eastern edges of the Tibetan Plateau and the Loess Plateau to China’s Pacific coast. In the CEC, four major regions of emission sources that exhibit haze pollution with excessive $PM_{2.5}$ concentrations and overall poor air quality are centered over the North China Plain (NCP), the Yangtze River Delta (YRD) in East China, the Pearl River Delta (PRD) in South China, and the Sichuan Basin (SCB) in Southwest China. As of late, severe haze pollution events that have swept over much of CEC have been attributed to the regional transport of air pollutants (Cheng et al., 2008; Deng et al., 2011; Qiao et al., 2019; Tie et al., 2017; Wang et al., 2016; Zhang et al., 2012). The regional transport of air pollutants with a source-receptor relationship is an important issue in our understanding of changes in air quality.

The source-receptor relationship of air pollution describes the impacts of emissions from an upwind source region to pollutant concentrations or deposition at a downwind receptor area (Seibert and Frank, 2004). The regional transport of source-receptor air pollutants is generally complicated by two types of factors: emissions and meteorology (Voulgarakis et al., 2010; Zhao et al., 2012). The emissions factor includes emission source strength, and chemical transformation and production. Meanwhile, the meteorological factor determines the transport pathway from the source to receptor regions, exchanges between the boundary layer and free troposphere, and the removal processes occurring over the source and receptor regions as well as along the transport pathways. Driven by atmospheric circulations, the regional transport of $PM_{2.5}$ from source regions can deteriorate air quality in the downwind receptor regions, leading to the regional haze pollution observed in a large area over China (Chang et al., 2018; He et al., 2017; Hu et al., 2018; Jiang et al., 2015; Wang et al., 2014).

The Yangtze River Middle Basin (YRMB) covers the lower subbasin of two provinces, Hubei and Hunan, in Central China. It is geographically surrounded by four major haze pollution regions, the NCP to the north, the YRD to the east, the PRD to the south, and the SCB to the west (Fig. 1a). Due to the specialized location of the YRMB as a regional air pollutant transport hub with subbasin topography (Fig. 1b), the regional transport of air pollutants driven by the cold air flows of East Asian winter monsoon over CEC can create a special source-receptor relationship between the source regions of haze pollution in upstream and the downwind YRMB region (Zhong et al., 2019). However, there are unresolved questions regarding the meteorological processes involved in the regional transport of air pollutants and the patterns of regional transport over CEC that may contribute to the air pollution changes observed in the YRMB area.

Wuhan, a metropolis located in the YRMB, has confronted environmental problems associated with urban air pollution, especially the heavy $PM_{2.5}$ pollution events that occur frequently in the winter (Gong et al., 2015; Xu et al., 2017). Local emissions of air pollutants from urban transportation, industrial exhaust, and bio-combustion play an important role in the YRMB urban air pollution (Acciai et al., 2017; Zhang et al., 2015). Previous observational and modeling studies on air pollution in this area have been conducted (Wu et al., 2018; Zheng et al., 2019). However, the regional transport routes of $PM_{2.5}$ across CEC are governed by meteorological drivers and their contribution to air pollution over the YRMB area are poorly understood, especially in relation to heavy air pollution events. This study selected Wuhan as a representative area within the YRMB for investigating the meteorological changes of air pollution events in January 2016 and assessing the contribution of regional transport of $PM_{2.5}$ over CEC to heavy air pollution in the YRMB area.

2. Data and methods

2.1 Data

Wuhan, the capital of the Hubei province, is located across the Yangtze River where its surrounding water network attributes to its humid environment (Fig. 1b). In order to analyze the air quality changes in Wuhan, hourly concentrations of air pollutants, including $PM_{2.5}$ in January 2016, were collected from the national air quality monitoring network operated by the Ministry of Ecology and Environment (http://www.mee.gov.cn/), including ten observational sites in Wuhan, nine of which were urban sites in residential and industrial zones and one which was suburban (Fig. S1). ~~The mass concentrations of surface $PM_{2.5}$ are operationally observed hourly with an instrument from Thermo Fisher Scientific.~~ The air quality observation data are released by the Ministry of Ecology and ~~Environment~~ Environmental Protection under quality control that is based on China's national standard of air quality observation.

The meteorological data of surface observations and air sounding in Wuhan and other observatories in CEC were obtained from the Meteorological Data Sharing Network of China Meteorological Administration (http://data.cma.cn/). The data selected for this study included air temperature, relative humidity, air pressure, and wind speed and wind direction. In order to analyze the meteorological variations in the atmospheric boundary layer at the time of our study, we used data with temporal resolutions of 3 h for surface observations, and 12 h for sounding observations.

The surface $PM_{2.5}$ concentrations, averaged over the ten observational sites in Wuhan, were used to characterize the variations of air pollution in January 2016 over this urban area. Correlation coefficients were calculated between the 10-site averages and the observed meteorological elements, including wind speed and air temperature, in Wuhan to explore the local meteorological influences on the changes of ambient $PM_{2.5}$ concentrations.

The ERA-Interim reanalysis data from the European Centre for Medium-Range Weather Forecasts (ECMWF) (https://www.ecmwf.int/en/forecasts/datasets/reanalysis-datasets/) were applied to explore the cold air flows of East Asian winter monsoonal winds in January 2016 and their anomalies during heavy $PM_{2.5}$ pollution over CEC.

2.2 FLEXPART-WRF modeling

2.2.1 Model description

The Flexible Particle dispersion (FLEXPART) model (Stohl et al., 2003; Stohl et al., 2005) is a Lagrange particle diffusion model developed by the Norwegian Institute for Air Research (NIAR). In this model, the trajectory of a large number of particles released from a source is simulated, considering the processes of tracer transport, turbulent diffusion, and wet and dry depositions in the atmosphere (Brioude et al., 2013). Applying a backward trajectory simulation can determine the distribution of potential source regions that may have an impact on a target point or receptor region (Chen et al., 2017a; Chen et al., 2017b; Seibert and Frank, 2004; Zhai et al., 2016).

Initially, the FLEXPART model could be driven by the global reanalysis meteorological data obtained from the ECMWF or the National Centers of Environmental Prediction (NCEP). However, since this study focuses on the fine and multiscale modeling of air pollutant sources and regional transport, the FLEXPART model was coupled offline with the Weather Research and Forecasting (WRF) model to effectively devise the combined model FLEXPART-WRF (Fast and Easter, 2006; Brioude et al., 2013), which has been widely used to investigate the potential sources of air pollutants regarding environmental change (An et al., 2014; De Foy et al., 2011; Sauvage et al., 2017; Stohl et al., 2003).

2.2.2 WRF modeling configuration and meteorological validation

In this study, the WRF model was configured with two nested domains, coarse and fine. The coarse domain covered the entirety of Asia with a 30 × 30 km horizontal resolution, and the nested fine domain included most of China and its surrounding regions with a 10 × 10 km horizontal resolution (Fig. S2). The physical parameterizations used in WRF modeling were selected with the Morrison microphysics scheme (Morrison et al., 2009), the Rapid Radiative Transfer Model (RRTM) scheme for long and short wave radiation (Mlawer et al., 1997), the Yonsei University (YSU) boundary layer scheme (Hong et al., 2006), the Grell 3D cumulus parameterization, and the Noah land surface scheme (Grell et al., 2005). Using the reanalysis meteorological data in the horizontal resolutions of 1°×1° obtained from NCEP for initial and boundary meteorological conditions, the WRF simulation ran 12 h each time, where the first 6 h simulations constituted spin-up time.

The WRF-simulated meteorological fields, which included wind speed and direction, air temperature, relative humidity, and air pressure, were compared with observations at five typical sites (Wuhan, Changsha, Hefei, Zhengzhou, and Nanchang) over CEC. The correlation coefficients were calculated and found to pass the significance level of 0.001, and the normalized standardized deviations were determined to be low (Taylor, 2001) (Fig. 2). Based on these results, it was evaluated that the WRF modeled meteorology was reasonably consistent with observations and could be used to drive the FLEXPART backward trajectory simulation.

2.3 Estimating contribution of regional transport of $PM_{2.5}$ to air pollution

In the FLEXPART-WRF model, the trajectory of particles released from a source is simulated. Using this Lagrangian method could result in a Jacobian matrix (footprint) with units of mass per volume per unit flux. Stohl et al (2005) mathematically derived the residence time for particles out of FLEXPART. Generally, in the backward trajectory of FLEXPART modeling, many particles are released at a receptor and transported backward in time. Then the residence time (not the lifetime) of all particles, normalized by the total number of released particles, is determined on a uniform grid. Selecting Wuhan as the receptor in the YRMB, the residence time for a thickness of 100 m above the surface was calculated and considered the ‘‘footprint’’ (in units of s). By multiplying the residence time with the air pollutant emission flux in the respective grid cell (in units of $\mu g\ m^{-2}\ s^{-1}$) calculated from the air pollutant emission inventory of 2016 for China (http://www.meicmodel.org/), the emission source contribution (in units of $\mu g\ m^{-2}$) from this grid cell to the receptor’s air pollution change could be estimated (Stohl et al., 2003; Stohl et al., 2005; Ding et al., 2009).

In this study, the FLEXPART-WRF simulation was conducted for a 48 h backward trajectory with the release of 50,000 air particles in the first h from Wuhan (30.61°N, 114.42°E) for three heavy pollution events in January 2016. The results were output with the residence time of air particles in a horizontal resolution of 0.1° × 0.1°. The simulations of particle residence time over the 48 h backward trajectory pathways were multiplied with the regional primary $PM_{2.5}$ emission fluxes to quantify the contribution of regional transport of $PM_{2.5}$ to air quality change in the YRMB area while identifying patterns of regional transport of $PM_{2.5}$ over CEC. The primary $PM_{2.5}$ emission data from the Multi-resolution Emission Inventory for China (MEIC) (http://www.meicmodel.org/) in 2016 were selected for use as the regional $PM_{2.5}$ emission fluxes in this study.

Based on this backward trajectory simulation, the upstream sources of $PM_{2.5}$ emissions for heavy air pollution in Wuhan were identified. The contribution rates $\boldsymbol{rate_{i,j}}$ of regional transport of

$PM_{2.5}$ from the upstream sources to air pollution in the downstream receptor region of the YRMB were calculated by Eq. (1), and the total contribution ***R*** of regional transport from the non-local emission sources are estimated by Eq. (2) (Chen et al., 2017b; Ding et al., 2009).

$$rate_{i,j} = \frac{E_{i,j} \times r_{i,j}}{\sum_{1,1}^{N,S} E_{i,j} \times r_{i,j}} \qquad (1)$$

$$R = \sum_{(N_1,S_1)}^{(N_2,S_2)} rate_{i,j} \qquad (2)$$

where the subscripts ***i*** and **j** represent a grid location (***i, j***) over the 48 h backward trajectory from the first grid (***i***=1, ***j***=1) in Wuhan to the last grid (***i***=*N,* ***j***=*S*) over CEC; $\mathbf{r}_{\boldsymbol{i,j}}$ represents the residence time of $PM_{2.5}$ particles simulated by FLEXPART-WRF; and $E_{\boldsymbol{i,j}}$ represents the $PM_{2.5}$ emission flux over the grid. In Eq. (2), the first grid location (N_1, S_1) and the last grid location (N_2, S_2) over the non-local emission sources and the local area of Wuhan were determined, respectively, by the regional transport of $PM_{2.5}$ pathways and the YRMB area in Wuhan as simulated by the FLEXPART-WRF model.

3. Results and Discussion

3.1 Variations in local $PM_{2.5}$ concentrations and meteorology in January 2016

Based on the National Ambient Air Quality Standards of China released by the Ministry of Ecology and Environment in 2012 (http://www.mee.gov.cn/), light and heavy air pollution levels of $PM_{2.5}$ are categorized by the daily average $PM_{2.5}$ concentrations exceeding 75 and 150 μg m^{-3} in ambient air, respectively. The average monthly $PM_{2.5}$ concentration reached 105.8 μg m^{-3} in Wuhan, where the daily $PM_{2.5}$ concentrations exceeded 75 μg m^{-3} on 27 days during the entire month of January 2016 (Fig. 3a), indicating that this YRMB urban area was under significant

$PM_{2.5}$ pollution during this wintertime period. As shown in Figure 3a, a 21 day prolonged air pollution event resulted from high levels of daily $PM_{2.5}$ concentrations (> 75 μg m^{-3}) from the 1st to the 21st. During this period, three notably heavy air pollution events occurred on January 4th, the 10th to the 12th, and the 17th to the 18th with excessive daily $PM_{2.5}$ concentrations (>150 μg m^{-3}). These three events are marked as P1, P2, and P3, respectively (Fig. 3b). Based on these observations, we found the interesting phenomenon of an apparent approximately 7 day cycle of heavy air pollution, reflecting an important modulation of meteorological oscillation in the East Asian winter monsoonal winds affecting air pollution over the YRMB region (Xu et al., 2016a). A period analysis on long-term observation data of air quality could provide further understanding on air quality changes associated with meteorological drivers.

Figure 3b presents the hourly changes of $PM_{2.5}$ concentrations during the three heavy air pollution events P1, P2, and P3. P1 began at 11:00 a.m. (local time is used for all events) and ended at 11:00 p.m. the same day with an observed $PM_{2.5}$ concentration peak of 471.1 μg m^{-3}. P2 occurred from 10:00 p.m. on the 10th to 00:00 a.m. on the 12th. Over the 26 h duration, it had two peaks: 231.4 and 210.6 μg m^{-3}. P3 occurred between 7:00 p.m. on the 17th and 2:00 p.m. on the 18th with an explosive growth rate of 42.9 μg m^{-3} h^{-1}. These events were characterized by short durations of less than 26 h from rapid accumulation to fast dissipation.

The changes in $PM_{2.5}$ concentrations presented few differences between the suburban and urban sites. Both had similar patterns and peaks of hourly changes during the heavy pollution periods (Figs. S3, S4, and S5), demonstrating that regional heavy air pollution in a large area of the YRMB region is, in part, due to regional transport over CEC. The only obvious differences in air pollutant concentrations were measured during the clean air periods ($PM_{2.5}$ concentration < 75 μg m^{-3}) with the relative high and low concentrations of $PM_{2.5}$ at urban and suburban sites, respectively (Figs. S3, S4, and S5). This shows the important influence of high air pollutant emissions over urban areas on local air quality.

~~3.2 Meteorological influences on $PM_{2.5}$ changes in Wuhan~~

Using the environmental and meteorological data observed in Wuhan in January 2016, the effects of the meteorological conditions on $PM_{2.5}$ concentrations in the YRMB region were statistically analyzed in regard to hourly variations of surface $PM_{2.5}$ concentrations, near-surface wind speed (WS), wind direction (WD), surface air temperature (T) and pressure (P), and relative humidity (RH) (Fig. 4). Among the observed changes shown in Figure 4, the changes of $PM_{2.5}$ concentrations were found to have obviously positive correlations to T and RH, as well as a pronounced negative correlation to P and a weak positive correlation to WS (Table 1). There are several reasons for these results. Firstly, the lower WS could alter the concentrations of air pollutants with a weaker advection of cold air in conjunction with strong subsidence and stable atmospheric stratification, thus easily producing a stagnation area in the lower troposphere and resulting in regional pollutant accumulations for the development of haze events. Secondly, in the presence of high soil moisture, strong surface evaporation could increase the near-surface RH, which is conducive to the hygroscopic growth of participles for haze formation (Dawson et al., 2014; Xu et al., 2016a). Additionally, high air temperature and strong solar radiation could enhance chemical conversions for the formation of secondary aerosols in the atmosphere (He et al., 2012; Huang et al., 2014). Furthermore, precipitation could impact the emissions and depositions of air pollutants (Dawson et al., 2007; Cheng et al., 2016). These observations could reflect the special influences of meteorological factors, such as winds, air temperature, humidity, and precipitation, on the physical and chemical processes in the ambient atmosphere that affect air quality change in the YRMB region.

3.2 A unique meteorological condition of "non-stagnation" for heavy $PM_{2.5}$ pollution

3.2.1 Strong northerly winds

When we focused on the meteorological changes leading to high $PM_{2.5}$ levels exceeding 150 μg m^{-3} during the heavy air pollution events, it is noteworthy that all three episodes, P1, P2, and P3, were accompanied with strong WSs in the northerly direction, as well as evident turning points in prevailing conditions leading to falling T and increasing P (Fig. 4). The conditions observed during these episodes present the typical meteorological characteristics of cold air invasion with high air pressure over the East Asian monsoon region. The southward advance of a cold front could drive the regional transport of air pollutants over CEC (Kang et al., 2019). Climatologically, a strong northerly wind, low air temperature, and high air pressure are typical features of an incursion of cold air during the East Asian winter monsoon season that could disperse air pollutants, thus improving air quality in the NCP region (Miao et al., 2018; Xu et al., 2016b). This differs from the meteorological conditions of stagnation with weak winds observed for heavy air pollution events in the major air pollution regions of CEC (Ding et al., 2017;Huang et al., 2018), and the strong near-surface wind that anomalously accompanied the intensification of $PM_{2.5}$ during heavy air pollution periods over the study area (Fig. 4). This could imply that the regional air pollutant transport is worsening air quality over the YRMB, driven by the strong northerly winds during the East Asian winter monsoon season.

3.3 A unique meteorological condition of "non-stagnation" for heavy $PM_{2.5}$ pollution

To further investigate the connection between meteorological elements in the near-surface layer and changes in air quality affected by $PM_{2.5}$ concentrations in the YRMB region, we carried out a more detailed correlation analysis of $PM_{2.5}$ concentrations in Wuhan with WS and air temperature for three different levels of $PM_{2.5}$ concentrations: clean air environment ($PM_{2.5} < 75$ μg m^{-3}), light air pollution (75 μg $m^{-3} \leq PM_{2.5} < 150$ μg m^{-3}) and heavy air pollution ($PM_{2.5} \geq 150$ μg m^{-3}) periods (Table 2). The surface $PM_{2.5}$ concentrations were positively correlated with air temperature, and negatively correlated with wind speeds during the periods of clean air environment and light air pollution. It should be emphasized here that a significantly negative correlation ($R = -0.19$) of $PM_{2.5}$ concentrations to WS for the light air pollution period could indicate that weak winds are favorable for local $PM_{2.5}$ accumulation, reflecting an important effect of local air pollutant emissions on light air pollution periods over the YRMB area. In January 2016, the overall wind speed of Wuhan was weak with a monthly mean value of 2.0 m s^{-1}, which could help maintain the high $PM_{2.5}$ levels in the prolonged air pollution events experienced in the YRMB area. However, a significantly positive correlation ($R = 0.41$) existed between heavy air pollution levels of $PM_{2.5}$ concentrations ($PM_{2.5} > 150$ μg m^{-3}) and strong WSs during the heavy air pollution periods, which was inconsistent with the meteorological conditions of stagnation observed in the near-surface layer where weak winds were associated with heavy air pollution in East China (Cao et al., 2012; Deng et al., 2011). The meteorology and environment conditions in the YRMB region indicate the close association of heavy air pollution periods enhancing $PM_{2.5}$ concentrations with strong winds (Fig. 4, Table 2), therefore, reflecting a key role of regional transport of air pollutants in the development of the YRMB's heavy air pollution periods.

In order to clearly illustrate the impact of wind speed and direction on the $PM_{2.5}$ concentrations associated with the regional transport of upwind air pollutants, Figure 5 presents the relation of hourly changes in surface $PM_{2.5}$ concentrations to WS and wind direction in Wuhan during January 2016. As seen in Figure 5, strong northerly winds accompanied extremely high $PM_{2.5}$ concentrations (> 150 μg m^{-3}) during the heavy air pollution periods, including a northeast gale exceeding 5 m s^{-1} during the extreme heavy pollution periods with extremely high $PM_{2.5}$ concentrations (> 300 μg m^{-3}). These results reveal a unique meteorological condition of "non-stagnation" with strong winds during events of heavy air pollution over the YRMB area. Conversely, the observed $PM_{2.5}$ concentrations ranging between 75 and 150 μg m^{-3} for light air pollution periods generally corresponded with low wind speeds (< 2 m s^{-1}) (Fig. 5). Therefore, it is the meteorological condition of stagnation, characterized by weak winds, involved in the accumulation of local air pollutants that is responsible for the light air pollution periods. Meteorological impacts on air quality could include not only the stagnant condition of meteorology with weak winds and stable boundary layer but also air temperature, humidity, precipitation, and atmospheric radiation in close connection with atmospheric physical and chemical processes. The meteorological drivers of air quality change are complicated by a series of physical and chemical processes in the atmosphere, especially the formation of secondary air pollutants with strong hygroscopic growth in the humid air environment overlying the dense water network (Fig. 1b) in the YRMB region (Cheng et al., 2014; He et al., 2012; Huang et al., 2014).

3.2.2 unstable structures in the atmospheric boundary layer

The air sounding data observed in Wuhan were used to compare the structures of the atmospheric boundary layer during the heavy air pollution and clean air periods. Figure 6 presents the vertical profiles of air temperature, wind velocity, and potential temperature averaged for the heavy $PM_{2.5}$ pollution and clean air periods in January 2016. It can be seen that the inversion layer of air temperature did not exist during the heavy pollution periods, while a near-surface inversion layer appeared at the height of about 200 m during the clean air periods (Fig. 6a). Compared to the clean air period, the heavy air pollution events had stronger winds within the 1000 m layer but weaker winds above the 1000 m layer (Fig. 6b), indicating that the regional transport of $PM_{2.5}$ was mainly limited to the 1000 m layer, especially between 250 m and 800 m. These vertical structures of horizontal wind could conduce to the downward mixing of the regionally transported air pollutants and produce the near-surface accumulations of air pollutants over the YRMB area with elevated ambient $PM_{2.5}$ concentrations, thus contributing to heavy air pollution.

To quantitatively characterize the stability of the atmospheric boundary layer, the vertical profiles of potential air temperature (θ) were calculated with air temperature and pressure (Fig. 6c). In this study, the vertical change rate of θ was used to quantify the static stability of the boundary layer (Oke, 2002). A lower vertical change rate of θ generally indicates decreasing stability or increasing instability of the boundary layer. The averaged static stability values of the near-surface layer below a height of 200 m during the heavy pollution and clean air periods were approximately 4.4 and 13.2 K km^{-1}, respectively (Table 3). This obvious decrease in stability of the boundary layer from clean air to heavy pollution periods indicates an anomalous tendency of the unstable boundary layer for the heavy pollution periods during January 2016 in the YRMB area.

The meteorological conditions of stagnation characterized by weak wind, temperature inversion, and a stable vertical structure of the atmospheric boundary layer are generally accepted as the typical meteorological drivers for heavy air pollution (An et al., 2019; Ding et al., 2017). Nevertheless, this study revealed a unique meteorological condition of "non-stagnation" in the atmospheric boundary layer during heavy air pollution periods characterized by strong wind, lack of an inversion layer, and a more unstable structure of the atmospheric boundary layer. These "non-stagnant" meteorological conditions could be generally regarded as the typical pattern of atmospheric circulation that facilitates the regional transport of air pollutants from upstream sources to downwind receptor regions. The regional transport of $PM_{2.5}$ connected with the source-receptor relationship between the air pollution regions in CEC and the YRMB area was further investigated with the following observational and modeling analyses.

3.43 ChangesRegional transport of $PM_{2.5}$ andin northerly winds observed over CEC

The monthly averages of $PM_{2.5}$ concentrations and the anomalies of wind speed averaged in three heavy air pollution periods relative to the monthly mean wind speed in January 2016 observed over CEC are exhibited in Figure 7. Note that a large area of CEC experienced air pollution with high levels of $PM_{2.5}$ > 75 μg m^{-3} that were especially severe in the NCP region and the Fenhe-Weihe Plain in Central China (Fig. 7a). As seen in Figure 7, Wuhan (site 1 in Fig. 7a) and the surrounding YRMB region were situated in the downwind southern edge of the air pollution area blanketing CEC (Fig. 7a), where the northerly winds prevailed (Fig. 7b). Climatologically, CEC is a typical region of East Asian monsoons dominated with wintertime northerly winds (Ding, 1993). Note that the anomalously stronger northerly winds were observed over upstream CEC during the three periods of wintertime heavy $PM_{2.5}$ pollution (Fig. 7b). Driven by the stronger northerly winds, the regional transport of air pollutants from the source regions in windward CEC could largely contribute to heavy air pollution in the downwind receptor region of YRMB.

In order to explore the connection between the regional transport of $PM_{2.5}$ over CEC and the three events of heavy air pollution in the YRMB region, six observational sites were selected from the northwestern, northern, and northeastern directions over upstream CEC (Fig. 7a). These sites represent three different routes of the regional transport of $PM_{2.5}$ to Wuhan (site 1 in Fig. 7a) and are governed by the southward incursion of stronger northerly winds (Fig. 7b). Figure 8 presents the temporal changes of $PM_{2.5}$ concentration and wind speed along three typical routes of regional transport of $PM_{2.5}$ over CEC. The southeastward movement of heavy $PM_{2.5}$ pollution was driven by stronger northerly winds from Luoyang and Xinyang to Wuhan (sites 3, 2, and 1 in Fig. 7) and presented a northwestern route of regional transport of $PM_{2.5}$ for P1 (see upper panels of Fig. 8). The westward advance of $PM_{2.5}$ peaks was governed by the northeastern winds from Tongling and Hefei to Wuhan (sites 6, 5, and 1 in Fig. 7a). The regional transport of $PM_{2.5}$ across Eastern China to the YRMB in Central China exerted a significant impact on P2 (see middle panels of Fig. 8). A northern pathway of regional transport of $PM_{2.5}$ connected Zhengzhou and Xinyang to Wuhan (sites 4, 2, and 1 in Fig. 7a) during P3 with anomalously strong northerly winds (see Fig. 7b and lower panels of Fig. 8). Note, in Figure 8, that the heavy $PM_{2.5}$ pollution periods at the upstream sites of Hefei, Tongling, Luoyang, Xinyang, and Zhengzhou (sites 2-6 in Fig. 7a) were generally dispelled by strong northerly winds. At the same time, these winds could trigger the periods of heavy $PM_{2.5}$ pollution in the YRMB region (Wuhan, site 1 in Fig. 7a). Such inverse effects of strong winds on heavy air pollution in CEC and the YRMB region show the important role that regional transport of air pollutants can have in cleaning and worsening air pollution in the upstream CEC source regions and the downstream YRMB receptor region, respectively.

The regional transport over CEC that is associated with the source-receptor relationship directing heavy $PM_{2.5}$ pollution to the YRMB region was revealed via observational analysis. The FLEXPART-WRF backward trajectory modeling was used to further identify the patterns of regional transport of $PM_{2.5}$ and estimate the resulting contribution to heavy air pollution in the YRMB region in the following section.

3.~~5~~4 Contribution of regional transport of $PM_{2.5}$ to heavy pollution

In this study, for the receptor of Wuhan, the $PM_{2.5}$ contributions of regional transport over CEC to air pollution in the downwind receptor region could be approximately estimated. These estimations were based on the product of the residence time of air particles during regional transport as simulated by the FLEXPART-WRF model, and the $PM_{2.5}$ emission flux over the source grid in CEC determined by Eq. (1). The data yielded a so-called potential source contribution map, which is the geographical distribution of the regional transport contribution rates (%) of the emission source grid cell to $PM_{2.5}$ pollution at the receptor of Wuhan (Fig. 9).

The non-local emission sources that affected $PM_{2.5}$ concentrations during P1, P2, and P3 were quantified over CEC using the $PM_{2.5}$ contribution rates calculated with Eq. (1). Combining the distribution of high $PM_{2.5}$ contribution rates with the prevailing winds experienced during the three heavy $PM_{2.5}$ pollution periods, the major pathways of regional transport of $PM_{2.5}$ over CEC could be recognized (Fig. 9). During P1 in the YRMB region, the regional transport of air pollutants was centered along a northwestern route from the Fenhe-Weihe Plain in Central China, and a northeastern route from the YRD region in Eastern China (Fig. 9a). The YRD emission sources of air pollutants exerted a large impact on P2 through regional transport of $PM_{2.5}$ across Eastern China to the YRMB region along the north side of Yangtze River (Fig. 9b). Two major regional transport pathways of $PM_{2.5}$ indicated by the spatial distribution of high contribution rates of $PM_{2.5}$ from the NCP and YRD regions contributed to the elevated $PM_{2.5}$ concentrations during P3 (Fig. 9c). Governed by the anomalous northerly winds in January 2016 (Fig. 7b), the regional transport of $PM_{2.5}$ from the air pollutant emission source regions in CEC provided a significant contribution to the wintertime heavy $PM_{2.5}$ pollution observed in the YRMB region (Figs. 7-9). This was confirmed by the results of the FLEXPART-WRF backward trajectory simulation utilized in this study.

The $PM_{2.5}$ contributions of regional transport over CEC to the $PM_{2.5}$ concentrations during P1, P2, and P3 in the YRMB area were estimated using Eq. (2) with the resulting high contribution rates of 68.1%, 60.9%, and 65.3%, respectively (Table 4). The regional transport of $PM_{2.5}$ from non-local air pollutant emissions could contribute more than 65% of the $PM_{2.5}$ concentrations to the heavy air pollution in the YRMB region during the study period, revealing a large contribution of regional transport of $PM_{2.5}$ over CEC to the enhancement of $PM_{2.5}$ levels in the YRMB area for the wintertime heavy air pollution.

Note that the potential source contribution is estimated based on transport alone, ignoring chemical and removal processes. We understand that these processes, including complex deposition, and chemical conversion for the formation of secondary particles, were not introduced in the FLEXPART-WRF simulation, which could represent the basic features of contribution and patterns of regional $PM_{2.5}$ transport over CEC when limited to the primary $PM_{2.5}$ particles highlighted in this study.

Normally researchers rely on 3-D numerical models with process analysis capability, such as integrated process rates (IPRs), in order to quantify the contributions of regional transport to the occurrence of air pollution episodes. In this study, simulations with a Lagrange particle dispersion FLEXPART-WRF model were utilized to calculate the percentage contribution of regional transport while identifying the transport pathway. The major uncertainty of this method for such calculations, as compared to other methods such as IPRs, is that the physical and chemical processes, including chemical conversion for the formation of secondary particles, were not introduced in the FLEXPART-WRF simulation. Considering that there is less precipitation in the winter monsoon season over CEC, this methodology has proven its robustness to quantify the regional transport contribution within the uncertainty range by relying on a portion of secondary organic and inorganic aerosols that resulted from the complex physical and chemical processes in the atmosphere.

4. Conclusions

This study investigated the ambient $PM_{2.5}$ variations over Wuhan, a typical YRMB area in Central China in January 2016, by analyzing the observational data of the environment and meteorology. In addition to this, we did a FLEXPART-WRF simulation to explore the meteorological processes involved in the regional transport of air pollutants, the regional transport patterns of $PM_{2.5}$, and how it contributes to heavy air pollution in the YRMB region. Focusing our study on three heavy $PM_{2.5}$ pollution periods we found a unique “non-stagnant” atmospheric boundary layer for wintertime heavy air pollution that was aggravated by the regional transport of $PM_{2.5}$ over CEC. This boundary layer was characterized by strong winds, no inversion layer, and a more unstable structure. These non-stagnant conditions during heavy air pollution periods with high $PM_{2.5}$ concentrations facilitate our understanding of the air pollutant source-receptor relationship of regional transport in air quality change. Our study is of great interest to the air quality community given the unique features of the air pollution meteorology, which are very different from “stagnant” meteorological conditions presented in textbooks.

Although emissions and local accumulation of air pollutants can lead to the formation of light air pollution, in regard to $PM_{2.5}$ over the YRMB region, the regional transport of $PM_{2.5}$ from upstream source regions of air pollutant emissions in CEC contributed significantly (more than 65%) to the excessive $PM_{2.5}$ concentrations during wintertime heavy air pollution in the downwind YRMB region in January 2016, as governed by the strong northerly winds in the East Asian winter monsoon season over CEC.

Based on the variations of air quality and meteorology in a typical urban YRMB region, this study revealed a unique “non-stagnant” meteorological condition for heavy air pollution with a strong contribution of regional transport of $PM_{2.5}$ over China. These conditions and contributions can be investigated further with climate analyses of long-term observations and more comprehensive modeling of air quality and meteorology.

Data availability: The data used in this paper can be provided by Chao Yu (ychao012@foxmail.com) upon request.

Supplement: The supplement related to this article is available online at: https://doi.org/

Author contributions: CY, TZ, and YB conducted the study design. XY, LZ, and SK provided the observational data. LZ assisted with data processing. CY wrote the manuscript with the help of TZ and XY. YB, SK, JH, CC, JY, YY, GM, MW, and JC were involved in the scientific interpretation and discussion. All authors provided commentary on the paper.

Competing interests: The authors declare that they have no conflicts of interest.

Acknowledgement: This study was jointly funded by the National Natural Science Foundation of China (41830965; 91744209), the National Key R & D Program Pilot Projects of China (2016YFC0203304), and the Postgraduate Research & Practice Innovation Program of Jiangsu Province (KYCX18_1027).

References

Acciai, C., Zhang, Z., Wang, F., Zhong, Z., and Lonati, G.: Characteristics and source Analysis of trace Elements in $PM_{2.5}$ in the Urban Atmosphere of Wuhan in Spring, Aerosol and Air Quality Research, 17, 2224-2234, https://doi.org/10.4209/aaqr.2017.06.0207, 2017.

An, X., Yao, B., Li, Y., Li, N., and Zhou, L.: Tracking source area of Shangdianzi station using

Lagrangian particle dispersion model of FLEXPART, Meteorological Applications, 21, 466-473, https://doi.org/10.1002/met.1358, 2014.

An, Z., Huang, R. J., Zhang, R., Tie, X., Li, G., Cao, J., Zhou, W., Shi, Z., Han, Y., Gu, Z., and Ji, Y.: Severe haze in northern China: A synergy of anthropogenic emissions and atmospheric processes, Proceedings of the National Academy of Sciences, 116, 8657-8666, https://doi.org/10.1073/pnas.1900125116, 2019.

Brioude, J., Arnold, D., Stohl, A., Cassiani, M., Morton, D., Seibert, P., Angevine, W., Evan, S., Dingwell, A., Fast, J. D., Easter, R. C., Pisso, I., Burkhart, J., and Wotawa, G.: The Lagrangian particle dispersion model FLEXPART-WRF version 3.1, Geoscientific Model Development, 6, 1889-1904, https://doi.org/10.5194/gmd-6-1889-2013, 2013.

Cao, J.-j., Wang, Q.-y., Chow, J. C., Watson, J. G., Tie, X.-x., Shen, Z.-x., Wang, P., and An, Z.-s.: Impacts of aerosol compositions on visibility impairment in Xi'an, China, Atmospheric Environment, 59, 559-566, https://doi.org/10.1016/j.atmosenv.2012.05.036, 2012.

Chang, X., Wang, S., Zhao, B., Cai, S., and Hao, J.: Assessment of inter-city transport of particulate matter in the Beijing-Tianjin-Hebei region, Atmospheric Chemistry and Physics, 18, 4843-4858, https://doi.org/10.5194/acp-18-4843-2018, 2018.

Chen, B., Xu, X.-D., and Zhao, T.: Quantifying oceanic moisture exports to mainland China in association with summer precipitation, Climate Dynamics, 51, 4271-4286, https://doi.org/10.1007/s00382-017-3925-1, 2017a.

Chen, S., Zhou, G., and Zhu, B.: A method for fast quantification of air pollutant sources （in Chinese）, Acta Scientiae Circumstantiae, 37, 2474-2481, https://doi.org/10.13671/j.hjkxxb.2017.0045, 2017b.

Cheng, H., Gong, W., Wang, Z., Zhang, F., Wang, X., Lv, X., Liu, J., Fu, X., and Zhang, G.: Ionic composition of submicron particles ($PM_{1.0}$) during the long-lasting haze period in January 2013 in Wuhan, central China, Journal of Environmental Sciences, 26, 810-817, https://doi.org/10.1016/s1001-0742(13)60503-3, 2014.

Cheng, X., Zhao, T., Gong, S., Xu, X., Han, Y., Yin, Y., Tang, L., He, H., and He, J.: Implications of East Asian summer and winter monsoons for interannual aerosol variations over central-eastern China, Atmospheric Environment, 129, 218-228, https://doi.org/10.1016/j.atmosenv.2016.01.037, 2016.

Cheng, Y. F., Wiedensohler, A., Eichler, H., Heintzenberg, J., Tesche, M., Ansmann, A., Wendisch, M., Su, H., Althausen, D., and Herrmann, H.: Relative humidity dependence of aerosol optical properties and direct radiative forcing in the surface boundary layer at Xinken in Pearl River Delta of China: An observation based numerical study, Atmospheric Environment, 42, 6373-6397, https://doi.org/10.1016/j.atmosenv.2008.04.009, 2008.

Dawson, J., Adams, P., and Pandis, S.: Sensitivity of $PM_{2.5}$ to climate in the Eastern US: a modeling case study, Atmospheric chemistry and physics, 7, 4295-4309, https://doi.org/10.5194/acp-7-4295-2007, 2007.

Dawson, J. P., Bloomer, B. J., Winner, D. A., and Weaver, C. P.: Understanding the Meteorological Drivers of U.S. Particulate Matter Concentrations in a Changing Climate, Bulletin of the American Meteorological Society, 95, 521-532, https://doi.org/10.1175/bams-d-12-00181.1, 2014.

De Foy, B., Burton, S. P., Ferrare, R. A., Hostetler, C. A., Hair, J. W., Wiedinmyer, C., and Molina, L. T.: Aerosol plume transport and transformation in high spectral resolution lidar measurements and WRF-Flexpart simulations during the MILAGRO Field Campaign, Atmospheric Chemistry and Physics, 11, 3543-3563, https://doi.org/10.5194/acp-11-3543-2011, 2011.

Deng, J., Wang, T., Jiang, Z., Xie, M., Zhang, R., Huang, X., and Zhu, J.: Characterization of visibility and its affecting factors over Nanjing, China, Atmospheric Research, 101, 681-691, https://doi.org/10.1016/j.atmosres.2011.04.016, 2011.

Ding, A., Wang, T., Xue, L., Gao, J., Stohl, A., Lei, H., Jin, D., Ren, Y., Wang, X., and Wei, X.: Transport of north China air pollution by midlatitude cyclones: Case study of aircraft measurements in summer 2007, Journal of Geophysical Research: Atmospheres, 114, https://doi.org/doi:10.1029/2008JD011023, 2009.

Ding, Y.: Monsoons over china, Springer Science & Business Media, 1993.

Ding, Y., Wu, P., Liu, Y., and Song, Y.: Environmental and Dynamic Conditions for the Occurrence of Persistent Haze Events in North China, Engineering, 3, 266-271, https://doi.org/10.1016/j.eng.2017.01.009, 2017.

Fast, J. D., and Easter, R. C.: A Lagrangian particle dispersion model compatible with WRF, 7th WRF Users Workshop, NCAR, 2006, 19-22.

Fuzzi, S., Baltensperger, U., Carslaw, K., Decesari, S., Denier van der Gon, H., Facchini, M. C., Fowler, D., Koren, I., Langford, B., Lohmann, U., Nemitz, E., Pandis, S., Riipinen, I., Rudich, Y., Schaap, M., Slowik, J. G., Spracklen, D. V., Vignati, E., Wild, M., Williams, M., and Gilardoni, S.: Particulate matter, air quality and climate: lessons learned and future needs, Atmospheric Chemistry and Physics, 15, 8217-8299, https://doi.org/10.5194/acp-15-8217-2015, 2015.

Gong, W., Zhang, T., Zhu, Z., Ma, Y., Ma, X., and Wang, W.: Characteristics of $PM_{1.0}$, $PM_{2.5}$, and PM_{10}, and Their Relation to Black Carbon in Wuhan, Central China, Atmosphere, 6, 1377-1387, https://doi.org/10.3390/atmos6091377, 2015.

Grell, G. A., Peckham, S. E., Schmitz, R., McKeen, S. A., Frost, G., Skamarock, W. C., and Eder, B.: Fully coupled “online” chemistry within the WRF model, Atmospheric Environment, 39, 6957-6975, https://doi.org/10.1016/j.atmosenv.2005.04.027, 2005.

He, J., Mao, H., Gong, S., Yu, Y., Wu, L., Liu, H., Chen, Y., Jing, B., Ren, P., and Zou, C.: Investigation of Particulate Matter Regional Transport in Beijing Based on Numerical Simulation, Aerosol and Air Quality Research, 17, 1181-1189, https://doi.org/10.4209/aaqr.2016.03.0110, 2017.

He, K., Zhao, Q., Ma, Y., Duan, F., Yang, F., Shi, Z., and Chen, G.: Spatial and seasonal variability of $PM_{2.5}$ acidity at two Chinese megacities: insights into the formation of secondary inorganic aerosols, Atmospheric Chemistry and Physics, 12, 1377-1395, https://doi.org/10.5194/acp-12-1377-2012, 2012.

Hong, S.-Y., Noh, Y., and Dudhia, J.: A new vertical diffusion package with an explicit treatment of entrainment processes, Monthly weather review, 134, 2318-2341, https://doi.org/10.1175/MWR3199.1,2006, 2006.

Hu, J., Li, Y., Zhao, T., Liu, J., Hu, X.-M., Liu, D., Jiang, Y., Xu, J., and Chang, L.: An important mechanism of regional O_3 transport for summer smog over the Yangtze River Delta in eastern China, Atmospheric Chemistry and Physics, 18, 16239-16251, https://doi.org/10.5194/acp-18-16239-2018, 2018.

Huang, Q., Cai, X., Wang, J., Song, Y., and Zhu, T.: Climatological study of the Boundary-layer air Stagnation Index for China and its relationship with air pollution, Atmospheric Chemistry and Physics, 18, 7573-7593, https://doi.org/10.5194/acp-18-7573-2018, 2018.

Huang, R. J., Zhang, Y., Bozzetti, C., Ho, K. F., Cao, J. J., Han, Y., Daellenbach, K. R., Slowik, J.

G., Platt, S. M., Canonaco, F., Zotter, P., Wolf, R., Pieber, S. M., Bruns, E. A., Crippa, M., Ciarelli, G., Piazzalunga, A., Schwikowski, M., Abbaszade, G., Schnelle-Kreis, J., Zimmermann, R., An, Z., Szidat, S., Baltensperger, U., El Haddad, I., and Prevot, A. S.: High secondary aerosol contribution to particulate pollution during haze events in China, Nature, 514, 218-222, https://doi.org/10.1038/nature13774, 2014.

Jiang, C., Wang, H., Zhao, T., Li, T., and Che, H.: Modeling study of $PM_{2.5}$ pollutant transport across cities in China's Jing-Jin-Ji region during a severe haze episode in December 2013, Atmospheric Chemistry and Physics, 15, 5803-5814, https://doi.org/10.5194/acp-15-5803-2015, 2015.

Kang, H., Zhu, B., Gao, J., He, Y., Wang, H., Su, J., Pan, C., Zhu, T., and Yu, B.: Potential impacts of cold frontal passage on air quality over the Yangtze River Delta, China, Atmospheric Chemistry and Physics, 19, 3673-3685, https://doi.org/10.5194/acp-19-3673-2019, 2019.

Miao, Y., Guo, J., Liu, S., Zhao, C., Li, X., Zhang, G., Wei, W., and Ma, Y.: Impacts of synoptic condition and planetary boundary layer structure on the trans-boundary aerosol transport from Beijing-Tianjin-Hebei region to northeast China, Atmospheric Environment, 181, 1-11, https://doi.org/10.1016/j.atmosenv.2018.03.005, 2018.

Mlawer, E. J., Taubman, S. J., Brown, P. D., Iacono, M. J., and Clough, S. A.: Radiative transfer for inhomogeneous atmospheres: RRTM, a validated correlated-k model for the longwave, Journal of Geophysical Research: Atmospheres, 102, 16663-16682, https://doi.org/10.1029/97jd00237, 1997.

Morrison, H., Thompson, G., and Tatarskii, V.: Impact of Cloud Microphysics on the Development of Trailing Stratiform Precipitation in a Simulated Squall Line: Comparison of One- and

Two-Moment Schemes, Monthly Weather Review, 137, 991-1007, https://doi.org/10.1175/2008mwr2556.1, 2009.

Nel, A.: Air pollution-related illness: effects of particles, Science, 308, 804-806, https://doi.org/10.1126/science.1108752, 2005.

Oke, T. R.: Boundary layer climates, Routledge, 2002.

Qiao, X., Guo, H., Tang, Y., Wang, P., Deng, W., Zhao, X., Hu, J., Ying, Q., and Zhang, H.: Local and regional contributions to fine particulate matter in the 18 cities of Sichuan Basin, southwestern China, Atmospheric Chemistry and Physics, 19, 5791-5803, https://doi.org/10.5194/acp-19-5791-2019, 2019.

Sauvage, B., Fontaine, A., Eckhardt, S., Auby, A., Boulanger, D., Petetin, H., Paugam, R., Athier, G., Cousin, J.-M., Darras, S., Nédélec, P., Stohl, A., Turquety, S., Cammas, J.-P., and Thouret, V.: Source attribution using FLEXPART and carbon monoxide emission inventories: SOFT-IO version 1.0, Atmospheric Chemistry and Physics, 17, 15271-15292, https://doi.org/10.5194/acp-17-15271-2017, 2017.

Seibert, P., and Frank, A.: Source-receptor matrix calculation with a Lagrangian particle dispersion model in backward mode, Atmospheric Chemistry and Physics, 4, 51-63, https://doi.org/10.5194/acp-4-51-2004, 2004.

Stohl, A., Forster, C., Eckhardt, S., Spichtinger, N., Huntrieser, H., Heland, J., Schlager, H., Wilhelm, S., Arnold, F., and Cooper, O.: A backward modeling study of intercontinental pollution transport using aircraft measurements, Journal of Geophysical Research: Atmospheres, 108, https://doi.org/10.1029/2002jd002862, 2003.

Stohl, A., Forster, C., Frank, A., Seibert, P., and Wotawa, G.: Technical note: The Lagrangian particle dispersion model FLEXPART version 6.2, Atmospheric Chemistry & Physics, 5, 2461-2474, https://doi.org/10.5194/acp-5-2461-2005, 2005.

Taylor, K. E.: Summarizing multiple aspects of model performance in a single diagram, Journal of Geophysical Research: Atmospheres, 106, 7183-7192, https://doi.org/10.1029/2000jd900719, 2001.

Tie, X., Huang, R. J., Cao, J., Zhang, Q., Cheng, Y., Su, H., Chang, D., Poschl, U., Hoffmann, T., Dusek, U., Li, G., Worsnop, D. R., and O'Dowd, C. D.: Severe Pollution in China Amplified by Atmospheric Moisture, Science Report, 7, 15760, https://doi.org/10.1038/s41598-017-15909-1, 2017.

Voulgarakis, A., Savage, N., Wild, O., Braesicke, P., Young, P., Carver, G., and Pyle, J.: Interannual variability of tropospheric composition: the influence of changes in emissions, meteorology and clouds, Atmospheric Chemistry and Physics, 10, 2491-2506, https://doi.org/10.5194/acp-10-2491-2010, 2010.

Wang, H. L., Qiao, L. P., Lou, S. R., Zhou, M., Ding, A. J., Huang, H. Y., Chen, J. M., Wang, Q., Tao, S. K., Chen, C. H., Li, L., and Huang, C.: Chemical composition of $PM_{2.5}$ and meteorological impact among three years in urban Shanghai, China, Journal of Cleaner Production, 112, 1302-1311, https://doi.org/10.1016/j.jclepro.2015.04.099, 2016.

Wang, S. X., Zhao, B., Cai, S. Y., Klimont, Z., Nielsen, C. P., Morikawa, T., Woo, J. H., Kim, Y., Fu, X., Xu, J. Y., Hao, J. M., and He, K. B.: Emission trends and mitigation options for air pollutants in East Asia, Atmospheric Chemistry and Physics, 14, 6571-6603, https://doi.org/10.5194/acp-14-6571-2014, 2014.

Wu, J., Kong, S., Wu, F., Cheng, Y., Zheng, S., Yan, Q., Zheng, H., Yang, G., Zheng, M., Liu, D., Zhao, D., and Qi, S.: Estimating the open biomass burning emissions in central and eastern China from 2003 to 2015 based on satellite observation, Atmospheric Chemistry and Physics, 18, 11623-11646, https://doi.org/10.5194/acp-18-11623-2018, 2018.

Xu, G., Jiao, L., Zhang, B., Zhao, S., Yuan, M., Gu, Y., Liu, J., and Tang, X.: Spatial and Temporal Variability of the $PM_{2.5}/PM_{10}$ Ratio in Wuhan, Central China, Aerosol and Air Quality Research, 17, 741-751, https://doi.org/10.4209/aaqr.2016.09.0406, 2017.

Xu, J., Chang, L., Qu, Y., Yan, F., Wang, F., and Fu, Q.: The meteorological modulation on $PM_{2.5}$ interannual oscillation during 2013 to 2015 in Shanghai, China, Science of the Total Environment, 572, 1138-1149, https://doi.org/10.1016/j.scitotenv.2016.08.024, 2016a.

Xu, X., Zhao, T., Liu, F., Gong, S. L., Kristovich, D., Lu, C., Guo, Y., Cheng, X., Wang, Y., and Ding, G.: Climate modulation of the Tibetan Plateau on haze in China, Atmospheric Chemistry and Physics, 16, 1365-1375, https://doi.org/10.5194/acp-16-1365-2016, 2016b.

Zhai, S., An, X., Liu, Z., Sun, Z., and Hou, Q.: Model assessment of atmospheric pollution control schemes for critical emission regions, Atmospheric Environment, 124, 367-377, https://doi.org/10.1016/j.atmosenv.2015.08.093, 2016.

Zhang, F., Wang, Z. W., Cheng, H. R., Lv, X. P., Gong, W., Wang, X. M., and Zhang, G.: Seasonal variations and chemical characteristics of $PM_{2.5}$ in Wuhan, central China, Science of the Total Environment, 518-519, 97-105, https://doi.org/10.1016/j.scitotenv.2015.02.054, 2015.

Zhang, R., Li, Q., and Zhang, R.: Meteorological conditions for the persistent severe fog and haze event over eastern China in January 2013, Science China Earth Sciences, 57, 26-35, https://doi.org/10.1007/s11430-013-4774-3, 2013.

Zhang, X. Y., Wang, Y. Q., Niu, T., Zhang, X. C., Gong, S. L., Zhang, Y. M., and Sun, J. Y.:

Atmospheric aerosol compositions in China: spatial/temporal variability, chemical signature, regional haze distribution and comparisons with global aerosols, Atmospheric Chemistry and Physics, 12, 779-799, https://doi.org/10.5194/acp-12-779-2012, 2012.

Zhao, T., Gong, S., Huang, P., and Lavoué, D.: Hemispheric transport and influence of meteorology on global aerosol climatology, Atmospheric Chemistry & Physics Discussions, 12, https://doi.org/10.5194/acp-12-7609-2012, 2012.

Zhao, X. J., Zhao, P. S., Xu, J., Meng, W., Pu, W. W., Dong, F., He, D., and Shi, Q. F.: Analysis of a winter regional haze event and its formation mechanism in the North China Plain, Atmospheric Chemistry and Physics, 13, 5685-5696, https://doi.org/10.5194/acp-13-5685-2013, 2013.

Zheng, H., Kong, S., Wu, F., Cheng, Y., Niu, Z., Zheng, S., Yang, G., Yao, L., Yan, Q., Wu, J., Zheng, M., Chen, N., Xu, K., Yan, Y., Liu, D., Zhao, D., Zhao, T., Bai, Y., Li, S., and Qi, S.: Intra-regional transport of black carbon between the south edge of the North China Plain and central China during winter haze episodes, Atmospheric Chemistry and Physics, 19, 4499-4516, https://doi.org/10.5194/acp-19-4499-2019, 2019.

Zhong, J., Zhang, X., Wang, Y., Wang, J., Shen, X., Zhang, H., Wang, T., Xie, Z., Liu, C., Zhang, H., Zhao, T., Sun, J., Fan, S., Gao, Z., Li, Y., and Wang, L.: The two-way feedback mechanism between unfavorable meteorological conditions and cumulative aerosol pollution in various haze regions of China, Atmos. Chem. Phys., 19, 3287–3306, https://doi.org/10.5194/acp-19-3287-2019, 2019.

Table 1. Correlation coefficients between hourly $PM_{2.5}$ concentrations and near-surface meteorological elements WS (wind speed), T (air temperature), P (air pressure), and RH (relative humidity) in Wuhan in January 2016.

Correlation coefficients	WS	T	P	RH
$PM_{2.5}$	0.10	0.31	-0.47	0.20

Table 2. Correlation coefficients of $PM_{2.5}$ concentrations with wind speed (WS) and air temperature (T) in different air quality levels during the study period.

Air quality	$PM_{2.5}$ levels	Number of samples	WS	T
Clean	$PM_{2.5} < 75$ μg m^{-3}	73	-0.20	0.56
Light pollution	75 μg $m^{-3} \leq PM_{2.5} < 150$ μg m^{-3}	135	-0.19	0.15
Heavy pollution	$PM_{2.5} \geq 150$ μg m^{-3}	37	0.41	-0.08

Table 3. Atmospheric static stability below heights of 200 m in the boundary layer during heavy pollution and clean air periods with anomalies relative to the average over January 2016 in Wuhan.

Period	heavy pollution period	clean air period	monthly average
	($K\ km^{-1}$)	($K\ km^{-1}$)	($K\ km^{-1}$)
Static stability	4.4	13.2	8.6
Anomalies of stability	-4.2	4.6	-

Table 4. The relative contributions of regional transport over CEC to three $PM_{2.5}$ heavy pollution periods, P1, P2, and P3, in the YRMB with local contributions.

Contribution rates	P1	P2	P3	Averages
Regional transport	68.1%	60.9%	65.3%	65.1%
Local contribution	31.9%	39.1%	34.7%	34.9%

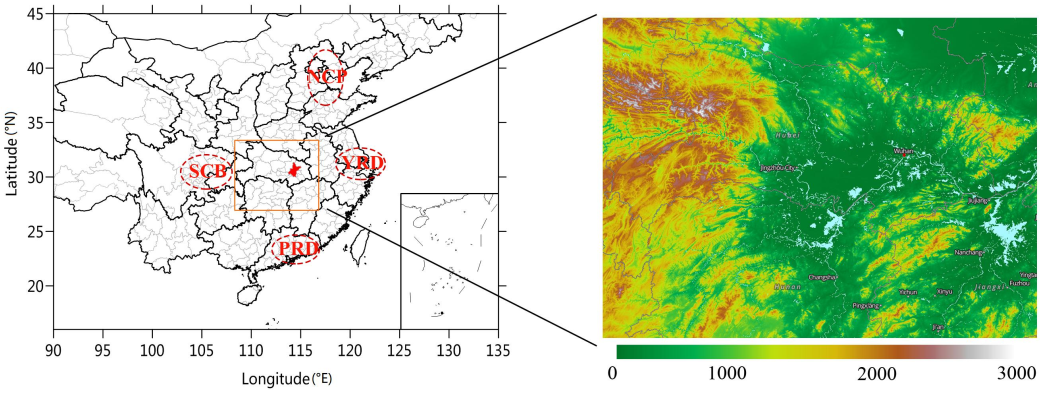

Fig. 1. (a) Distribution of the YRMB (orange rectangle) with the location of Wuhan (red area) and the major haze pollution regions of NCP, YRD, PRD, and SCB in CEC as well as (b) the YRMB region with terrain height (color contours, m in a.s.l.). The river and lake network (blue areas) are downloaded from https://worldview.earthdata.nasa.gov.

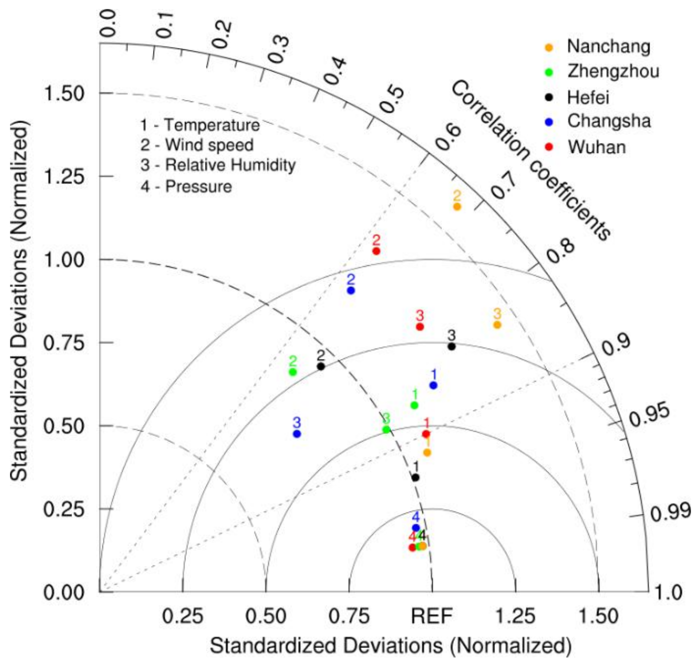

Fig. 2. A Taylor plot with the normalized standard deviations and correlation coefficients between WRF-simulated and observed meteorological fields. The radian of the sector represents the

correlation coefficient. The solid line indicates the ratio of standard deviation between simulations and observations. The distance from the marker to “REF” reflect the normalized root-mean-square error (NRMSE).

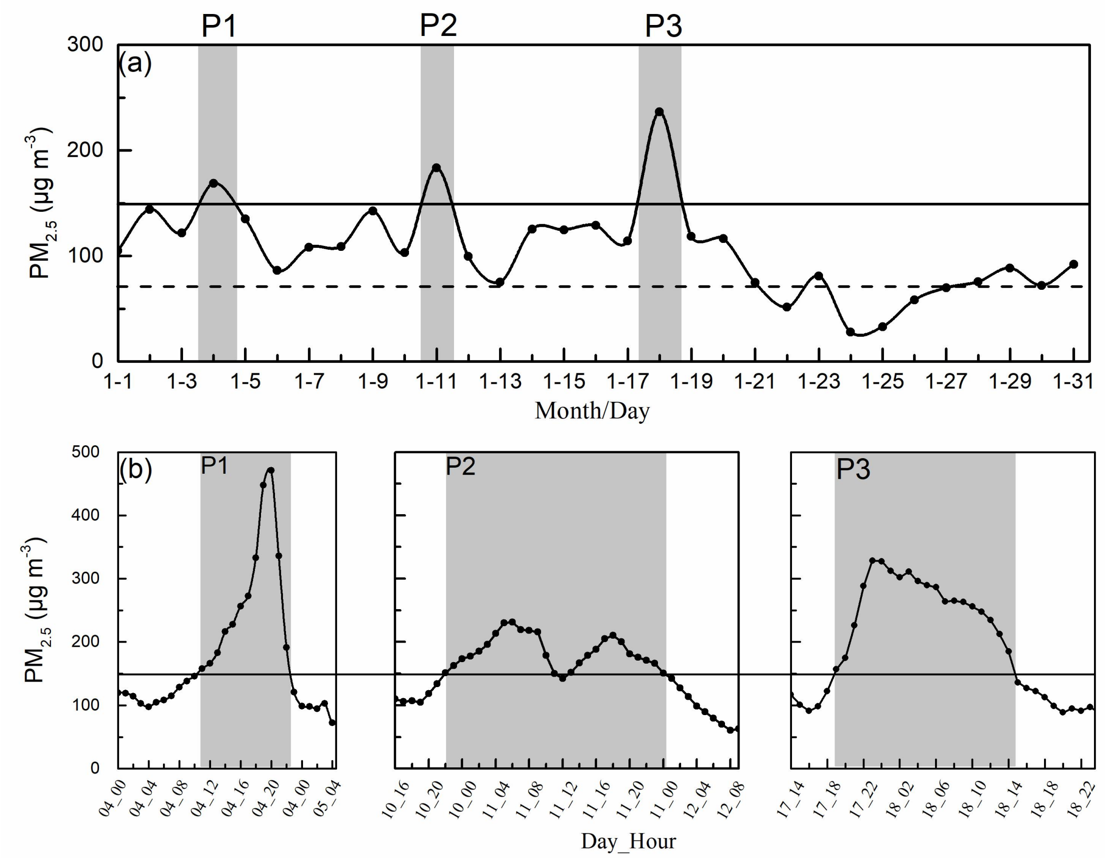

Fig. 3. (a) Daily changes of surface $PM_{2.5}$ concentrations in Wuhan in January 2016 with $PM_{2.5}$ concentrations exceeding 75 μg m^{-3} (dash line) and 150 μg m^{-3} (solid lines) for light and heavy haze pollution, respectively. (b) The hourly variations of surface $PM_{2.5}$ concentrations in three heavy air pollution events, P1, P2, and P3, with excessive $PM_{2.5}$ levels (> 150 μg m^{-3}) marked by the shaded areas.

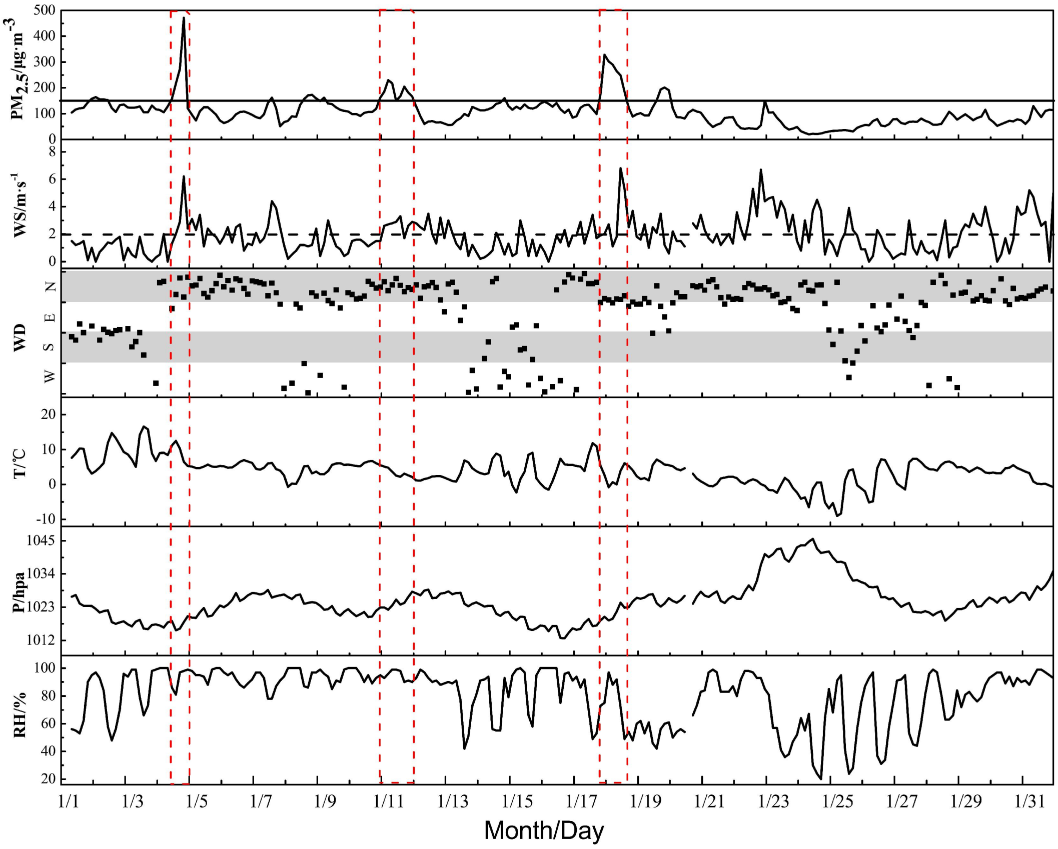

Fig. 4. Hourly variations of meteorological elements and $PM_{2.5}$ concentrations in Wuhan in January 2016. Heavy air pollution periods are marked with columns in red dash lines and $PM_{2.5}$ concentrations exceeding 150 μg m^{-3} (solid line in the upper panel).

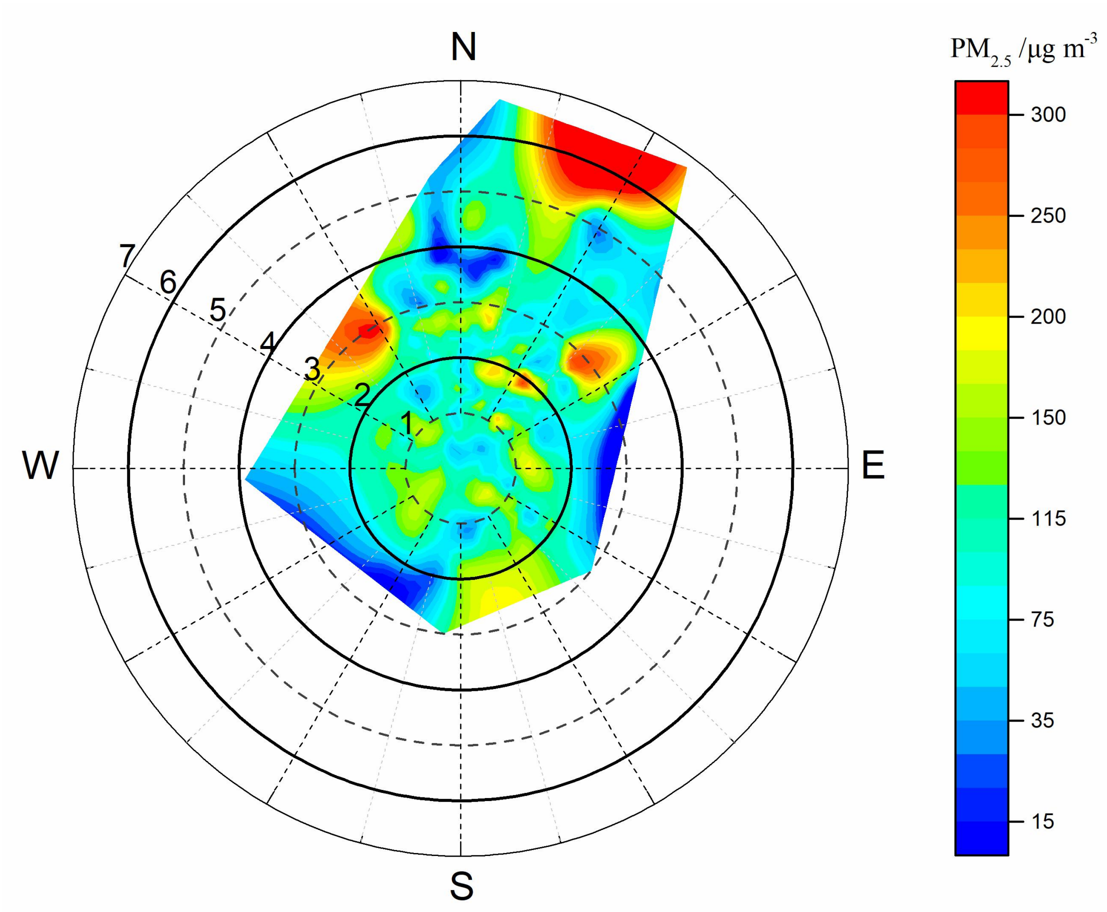

Fig. 5. A polar plot of the hourly variations in wind speed (round radius, in units of m s^{-1}) and direction (angles) to surface $PM_{2.5}$ concentrations (color contours, in units of µg m^{-3}) in Wuhan in January 2016.

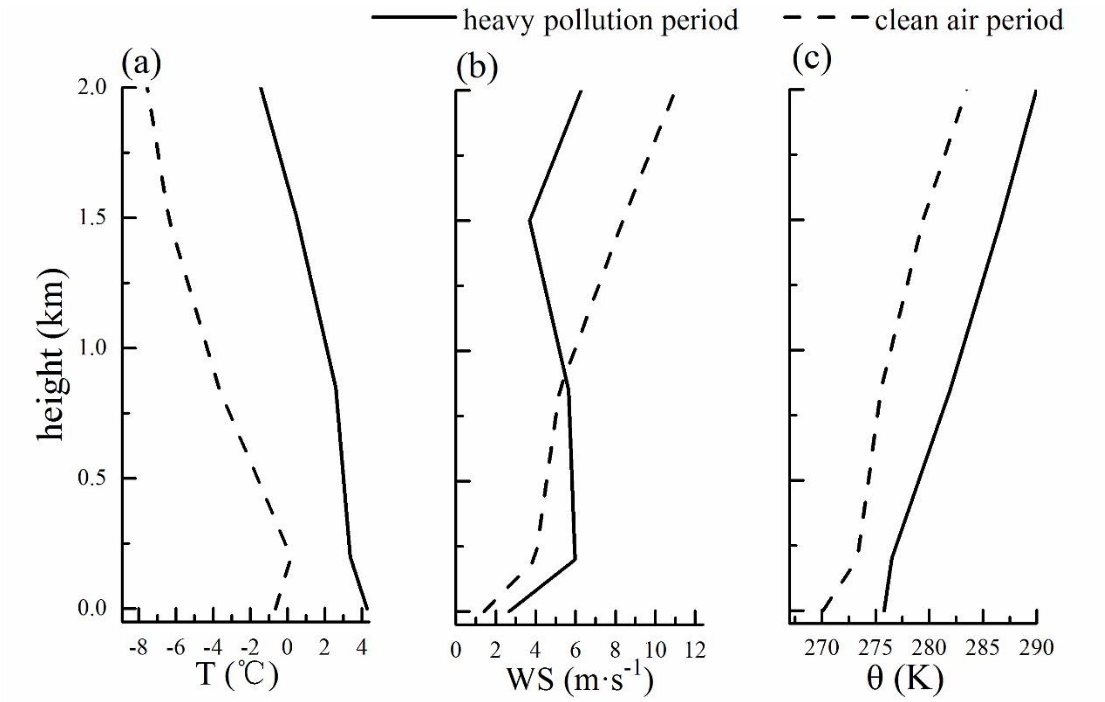

Fig. 6. Vertical profiles of (a) air temperature, (b) wind velocity and (c) potential temperature averaged in the heavy pollution periods P1, P2 and P3~~of heavy $PM_{2.5}$ pollution~~ and in the clean air period over Wuhan during January 2016.

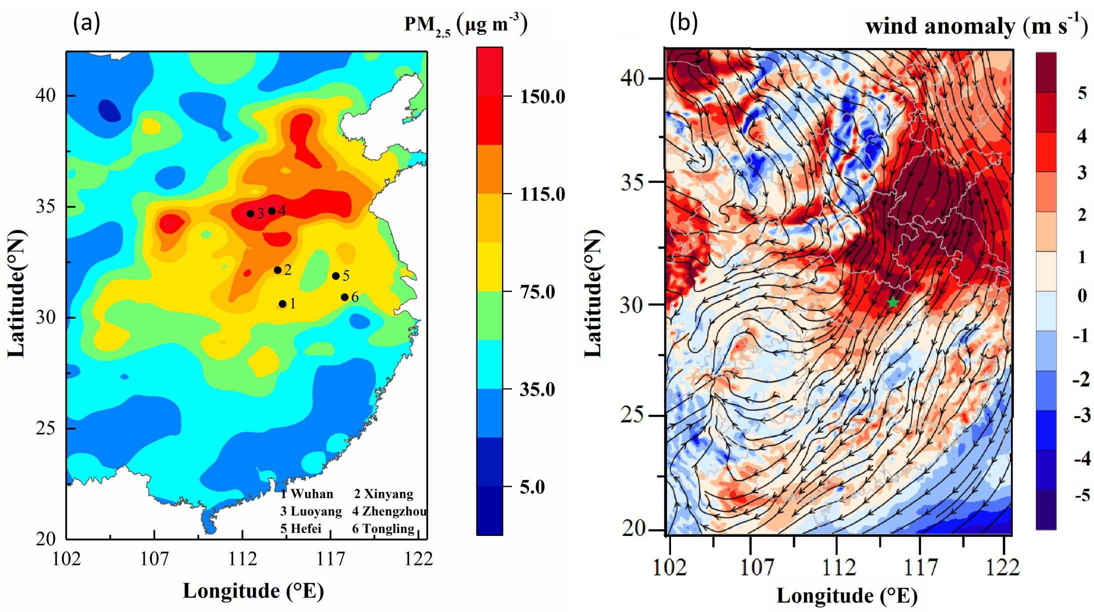

Fig. 7 (a) Distribution of the monthly averages of surface $PM_{2.5}$ concentrations observed in January 2016 over CEC with the locations of six sites (black dots): 1. Wuhan, 2. Xinyang, 3.

Luoyang, 4. Zhengzhou, 5. Hefei, and 6. Tongling. (b) Distribution of anomalies (color contours) of 200 m wind speeds averaged during the three heavy air pollution periods relative to the monthly wind averages (streamlines) in January 2016 over CEC with the location of Wuhan (a light blue star).

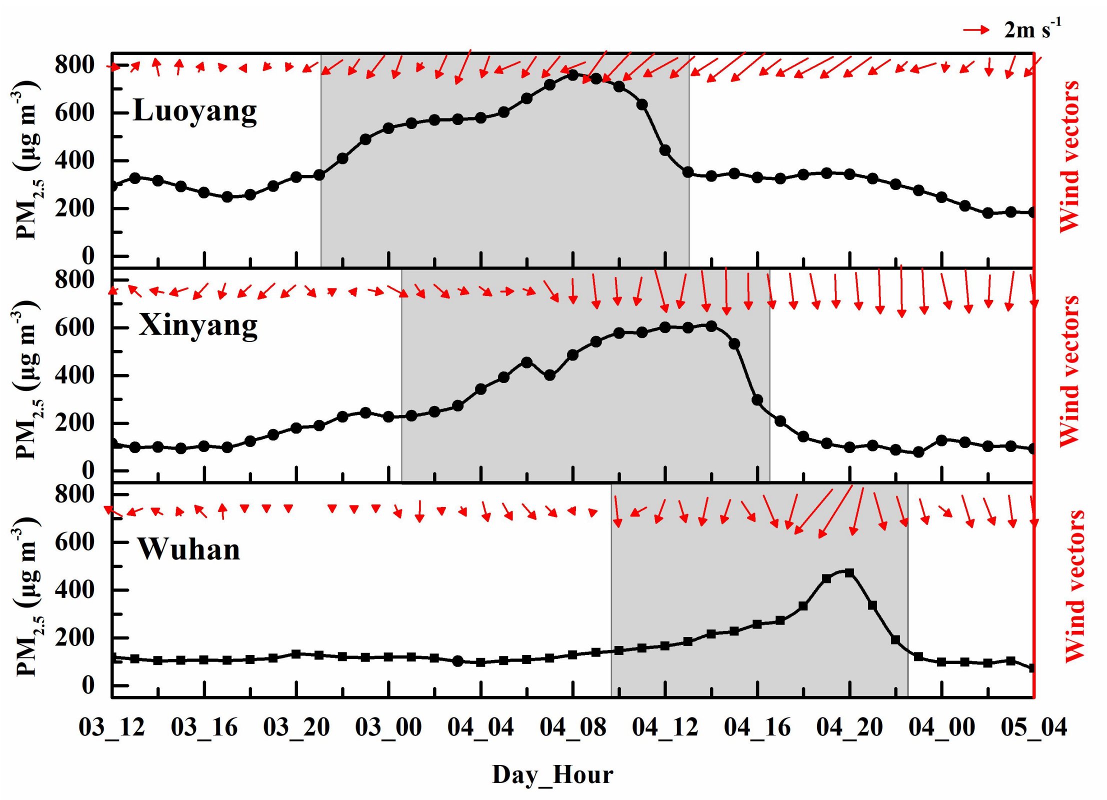

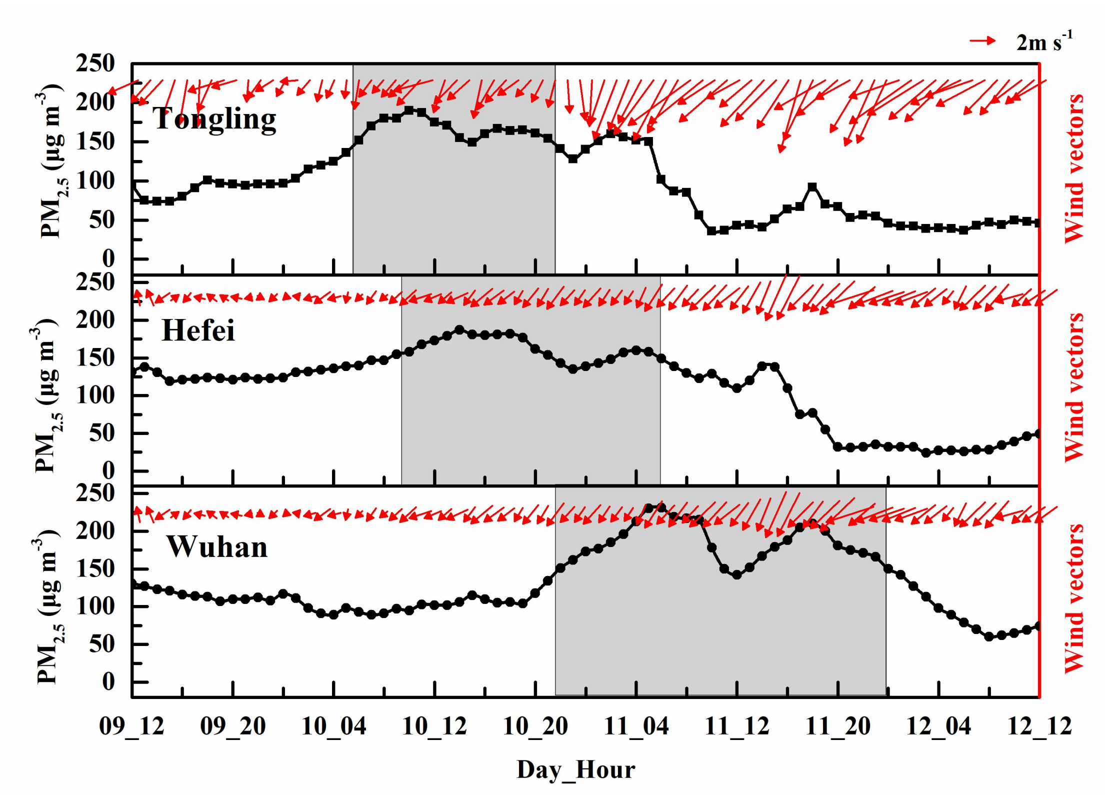

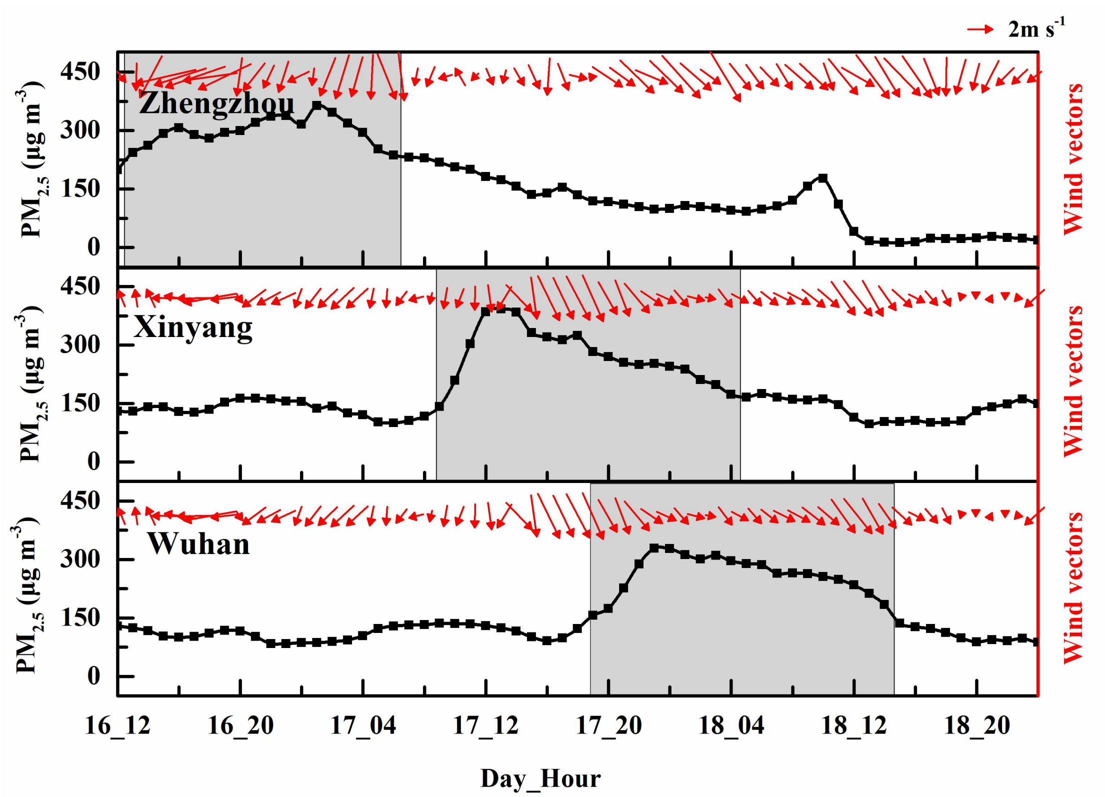

Fig. 8. Temporal changes of $PM_{2.5}$ concentrations (dotted lines) and near-surface winds (vectors) observed at five upstream sites (Fig. 6) and Wuhan with shifts of $PM_{2.5}$ peaks (marked with shaded

areas) to the YRMB's heavy $PM_{2.5}$ pollution periods P1 (upper panel), P2 (middle panel) and P3 (lower panel), in January 2016.

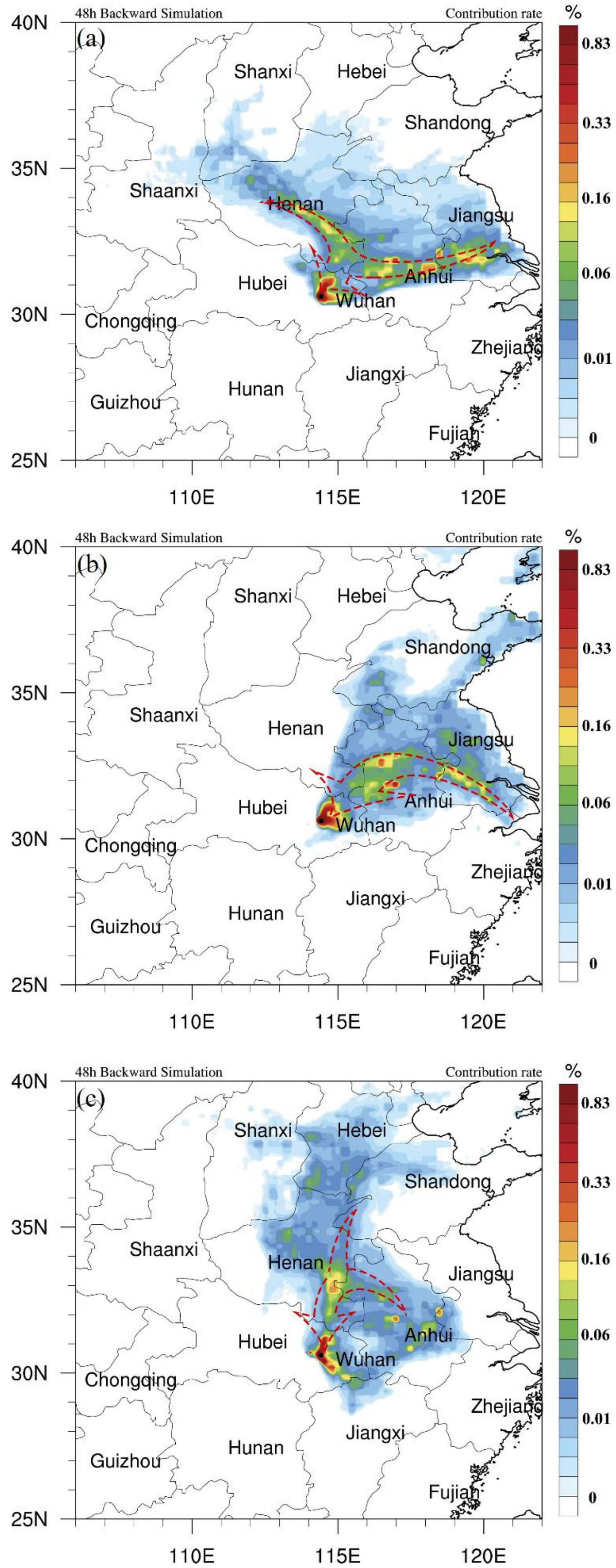

Fig. 9. Spatial distribution of contribution rates (color contours) to $PM_{2.5}$ concentrations in Wuhan

with the major pathways of regional transport over CEC (dash arrows) for three heavy pollution periods (a) P1, (b) P2, and (c) P3 in January 2016 simulated by the FLEXPART-WRF model.